Tellus (2005), 57B, 153–163
Printed in UK. All rights reserved

TELLUS

Increase of carbon cycle feedback with climate sensitivity: results from a coupled climate and carbon cycle model

By B. GOVINDASAMY[1]*, S. THOMPSON[1], A. MIRIN[1], M. WICKETT[1], K. CALDEIRA[1] and C. DELIRE[2†], [1]*Climate and Carbon Cycle Modeling Group, Lawrence Livermore National Laboratory, Livermore, CA 94550, USA;* [2]*Center for Sustainability and the Global Environment, Gaylord Nelson Institute for Environmental Studies, University of Wisconsin-Madison, Madison, WI 53726, USA*

(Manuscript received 7 April 2004; in final form 23 September 2004)

ABSTRACT

Coupled climate and carbon cycle modelling studies have shown that the feedback between global warming and the carbon cycle, in particular the terrestrial carbon cycle, could accelerate climate change and result in greater warming. In this paper we investigate the sensitivity of this feedback for year 2100 global warming in the range of 0 to 8 K. Differing climate sensitivities to increased CO_2 content are imposed on the carbon cycle models for the same emissions. Emissions from the SRES A2 scenario are used. We use a fully coupled climate and carbon cycle model, the INtegrated Climate and CArbon model (INCCA), the NCAR/DOE Parallel Climate Model coupled to the IBIS terrestrial biosphere model and a modified OCMIP ocean biogeochemistry model. In our integrated model, for scenarios with year 2100 global warming increasing from 0 to 8 K, land uptake decreases from 47% to 29% of total CO_2 emissions. Due to competing effects, ocean uptake (16%) shows almost no change at all. Atmospheric CO_2 concentration increases are 48% higher in the run with 8 K global climate warming than in the case with no warming. Our results indicate that carbon cycle amplification of climate warming will be greater if there is higher climate sensitivity to increased atmospheric CO_2 content; the carbon cycle feedback factor increases from 1.13 to 1.48 when global warming increases from 3.2 to 8 K.

1. Introduction

The physical climate system and the global carbon cycle are tightly coupled, as changes in climate affect exchange of atmospheric CO_2 with the land surface and ocean, and changes in CO_2 fluxes affect the Earth's radiative forcing and the physical climate system. During the 1980s, carbon uptake by oceans and terrestrial ecosystems each amounted to a quarter to a third of anthropogenic CO_2 emissions with strong interannual variability (Braswell et al., 1997; Prentice et al., 2000, 2001). A better understanding of carbon balance dynamics is required for interpreting variations in atmosphere-biosphere exchange (Fung et al., 1997) and for evaluating policies to mitigate anthropogenic CO_2 emissions (UNFCCC 1997; IGBP Terrestrial Carbon Working Group 1998).

Anthropogenic emissions of fossil fuels and change in land use are expected to lead to significant climate change in the future (IPCC, 2001). Both climate change and elevated CO_2 have an impact on land and ocean carbon uptake. Photosynthesis by plants will increase with increased atmospheric CO_2 content (the so-called CO_2 fertilization effect) when water and nutrients are available. Increased atmospheric CO_2 also promotes efficient use of water and nitrogen by plants, favouring growth in otherwise limiting situations (IPCC, 2001). However, the enhanced physiological effects of CO_2 on productivity and efficiency of water use are asymptotic at high CO_2 concentrations (King et al., 1997; Cao and Woodward, 1998). Increased global temperatures are expected to increase heterotrophic respiration rates, diminishing or even reversing the CO_2 flux from the atmosphere to the land biosphere (Cox et al., 2000; Friedlingstein et al., 2001; Cramer et al., 2001; Joos et al., 2001). Studies on ocean carbon uptake have suggested that global warming reduces the uptake of carbon by oceans also (Sarmiento and Le Quere, 1996; Sarmiento et al., 1998). This occurs primarily because CO_2 is less soluble in warmer water and increased stratification would tend to inhibit downward transport of anthropogenic carbon.

One way to study the feedbacks between the physical climate system and carbon cycles is to use three-dimensional (3-D) coupled ocean/atmosphere climate/carbon cycle general circulation

*Corresponding author.
e-mail: bala@llnl.gov
†Present address: Institut de Sciences de l'Evolution Universite Montpellier II, Place E. Bataillon 34095, Montpellier cedex 5, France.

models. Two such models have produced published results representing the dynamical response of the Earth's climate and carbon system to CO_2 emissions (Cox et al., 2000; Friedlingstein et al., 2001). The study by Cox et al. (2000) showed a very large positive feedback and the other study showed a much weaker feedback. A feedback analysis by Friedlingstein et al. (2003) indicated that the differences between the model results were due primarily to Southern Ocean circulation and the response of land carbon to global warming. However, land response to climate change was the dominant difference between the two model simulations of the 21st century. In the HadCM3 model (Cox et al., 2000), the land biosphere became a net source of CO_2 to the atmosphere, whereas in the IPSL model (Friedlingstein et al., 2001), the land biosphere was a net sink of CO_2 from the atmosphere.

Using the INtegrated Climate and CArbon (INCCA) model, Thompson et al. (2004) attempted to bracket uncertainty in terrestrial uptake arising from uncertainty in the land-biosphere CO_2 fertilization effect. They performed one simulation in which the land-biosphere model was very sensitive to CO_2 fertilization and another simulation in which the land uptake was restrained by limiting CO_2 fertilization at present-day levels. The fertilization-limited run was designed to represent the possibility that the CO_2 fertilization effect could saturate rapidly, perhaps due to nitrogen and/or nutrient limitations. Through to year 2100, the land was a very strong sink of carbon in the CO_2-fertilized simulation, but it became a source of carbon to the atmosphere in the fertilization-limited simulation by the year 2050. The predicted atmospheric CO_2 at year 2100 differed by 336 parts per million by volume (ppmv) (40%) between the two cases. In the fertilization-limited run, the vegetation biomass was stable but the soil carbon pool was shrinking because of climate change-induced increases in heterotrophic respiration. The authors showed that current uncertainties in CO_2 fertilization preclude determination of whether the land biosphere will amplify or damp atmospheric CO_2 increases by the end of the century.

The climate model used by Thompson et al. (2004) has a climate sensitivity ($\sim$2 K for a doubling of CO_2) near the low end of the conventionally accepted range (1.5 to 4.5 K per CO_2 doubling; IPCC, 2001). The land surface is more likely to damp the effects of CO_2 emissions if climate sensitivity is low, with carbon uptake by the biosphere dominated by CO_2 fertilization. Higher climate sensitivity is more likely to amplify the effect of CO_2 emissions, because increased respiration rates at higher temperatures would be expected to induce carbon losses from the land biosphere. In this study, we address the dependence of terrestrial and ocean carbon uptakes on climate sensitivity using the coupled climate and carbon cycle model of Thompson et al. (2004). The major purpose is to investigate the sensitivity of carbon cycle feedbacks to climate sensitivity. The range of climate change we have studied in this work is 0–8 K warming of global and annual mean surface temperature by the year 2100 for the SRES A2 scenario (IPCC, 2001). The warming produced here brackets the 1.4–5.8 K warming for the year 2100 projected by IPCC (2001). Our results are from a single modelling study, and intercomparison using other coupled climate and carbon cycle models is required.

2. Model

To investigate the sensitivity of the land and ocean carbon cycles to climate in the coupled climate system we used INCCA, a coupled climate and carbon cycle model (Thompson et al., 2004). The NCAR/DOE PCTM model (Meehl et al., 2004; Washington et al., 2000) was used as the physical ocean–atmosphere model; this is a version of the NCAR CCM 3.2 model (Kiehl et al., 1996) coupled to the LANL POP ocean model (Dukowicz and Smith, 1994; Maltrud et al., 1998). The climate model was coupled to a terrestrial biosphere model, Integrated Biosphere Simulator (IBIS) version 2 (Foley et al., 1996; Kucharik et al., 2000) and an ocean biogeochemistry model. The horizontal resolution of the land and atmosphere models is approximately 2.8° in latitude and 2.8° in longitude. The ocean model has a horizontal resolution of (2/3)°. The atmosphere and ocean models have 18 and 40 levels in the vertical, respectively.

Land surface biophysics, terrestrial carbon flux and global vegetation dynamics are represented in a single, physically consistent modelling framework within IBIS. IBIS simulates surface water, energy and carbon fluxes on hourly time steps and integrates them over the year to estimate annual water and carbon balance. The annual carbon balance of vegetation is used to predict changes in the leaf area index and biomass for each of 12 plant functional types which compete for light and water using different ecological strategies. IBIS also simulates carbon cycling through litter and soil organic matter. When driven by observed climatological datasets, the model's near-equilibrium run-off, net primary productivity (NPP) and vegetation categories show a fair degree of agreement with observations (Foley et al., 1996; Kucharik et al., 2000). We have parallelized IBIS to support both distributed and shared memory parallelism. The land points are partitioned among tasks in a load-balanced manner, with high-speed transposes used to connect the land and atmospheric domain decompositions.

In IBIS, the atmospheric CO_2 concentration affects photosynthesis mainly by affecting RuBp regeneration rates and Rubisco enzyme-catalysed carboxylation rates according to Farquhar et al. (1980) and Collatz et al. (1992). Higher CO_2 concentrations also reduce stomatal conductance following Ball et al. (1986) and Collatz et al. (1991, 1992), thereby improving efficiency of water use and drought resistance at the ecosystem level. Hence, the CO_2 fertilization effect in IBIS results from both changes in canopy physiology and ecosystem dynamics. On the other hand, increased atmospheric CO_2 also indirectly favours heterotrophic respiration as the increased NPP leads to increased litter fall and higher availability of organic substrates

for microbial activity. The nitrogen cycle and acclimation of soil microbiology to the higher temperatures (Kirschbaum, 2000; Tjoelker et al., 2001) are not explicitly taken into account in IBIS.

Compared with other dynamic vegetation models, IBIS tends to simulate a fairly strong fertilization effect (Cramer et al., 2001; McGuire et al., 2001). This can partly be explained by the fact that IBIS does not simulate the effect of nutrients limitations. Changes in competition at the ecosystem level in response to improved water-use efficiency and increased photosynthesis seem to play an important role too.

IBIS was designed to simulate the dynamics of natural vegetation and the carbon cycling within vegetation and soils. It does not take into account land use practices. In the series of simulations presented in the next section, we use estimates of the emissions due to land-use change for the historical period (Houghton, 2003) and a scenario for the 21st century. These estimates include among others the effect of conversion of natural ecosystems to cultivated lands and pastures, the harvest of wood, and the establishment of tree plantations. The effect of fire suppression in the United States is also included (Houghton, 2003). The effect of nutrient fertilization of crops is not included.

The ocean biogeochemistry model is based on the Ocean Carbon-cycle Intercomparison Project (OCMIP) biotic protocols (Najjar and Orr, 1999). This model predicts air–sea CO_2 fluxes, biogenic export of organic matter and calcium carbonate, and distributions of dissolved inorganic carbon, phosphate, oxygen, alkalinity and dissolved organic matter. In the OCMIP protocol, export of biogenic materials is computed to maintain observed upper ocean nutrient concentrations. However, because our simulations involve changes in ocean circulation, we cannot make the assumption that surface nutrient concentrations remain stationary. Therefore, we replaced the OCMIP export formulation with a formulation based on that of Maier-Reimer (1993):

$$J_{\mathrm{PROD}} = (1/\tau) g(\mathrm{PAR}) Q_{10}^{(\Delta T/10)} P^2/(P_{1/2} + P),$$

where J_{PROD} is the rate of phosphate uptake for production of both exported particulate organic matter and dissolved organic matter and τ is the time constant for removal of phosphate from the surface layer at 25°C in the case of sufficient nutrients and light (here taken to be 60 days). Light sensitivity of growth, g(PAR), is modelled according to Tian et al. (2000), temperature dependence of growth rate is modelled using $Q_{10} = 2$ following Wolf-Gladrow and Riebesell (1997) and P is the phosphate concentration; following Maier-Reimer (1993), we used a half saturation value for phosphate, $P_{1/2}$, of 2×10^{-5} mol m^{-3}.

Initial coupled simulations showed that when IBIS2 was coupled to the PCTM, precipitation biases typical of current climate models caused vegetation errors that, in turn, amplified precipitation biases in regions where surface–atmosphere moisture recycling is known to be important. This erroneous feedback resulted in unacceptable vegetation in some areas, particularly parts of the Amazon. To remedy this, a precipitation correction scheme was implemented. At every surface grid point, and every time step, the simulated precipitation field is multiplied by a constant that is a function of position but otherwise static and identical across all runs. The constant precipitation "correction field" acts to move the model's simulated present-day annual mean precipitation towards an observed climatology. However, we maintain the model's global conservation of water and energy. In effect the procedure spatially redistributes the model's precipitation at each time step.

Because it uses a fixed ratio, this precipitation correction has minimal impact on the model's daily and seasonal precipitation characteristics while allowing for global hydrological changes, i.e. a long-term precipitation change can still occur at any location. Thus the kind of feedback that produced a catastrophic Amazonian vegetation change in the run of Cox et al. (2000) can still occur. In practice, the precipitation correction employed here is similar to the surface heat "flux corrections" used in early coupled ocean–atmosphere models. It would be better not to have to use it, but until model improvements obviate the need, a correction is required to generate a reasonable coupled control case.

3. Experiments

We developed a year 1870 "pre-industrial" initial condition with more than 200 yr of fully coupled equilibration before the start of experiments. During the first half of the spin-up period, changes in soil carbon pools were accelerated by a factor of 40. We performed four model simulations starting from the pre-industrial initial conditions:

(1) The "control" case with no change in forcing for the period 1870–2100. Climate drift evaluated for the period 1900–2100 is a −0.35 K change in mean surface temperature (Table 1), about 6.4% growth in the extent of sea ice and a 3.14 ppmv increase in atmospheric CO_2 concentration. All are residuals from a slight imbalance in the initial state. Since the control drifts are minimal, they are not subtracted from the other simulations in our analysis.

(2) The "1 × sensitivity" case in which the radiative forcing of atmospheric CO_2 on the climate system is calculated based on predicted atmospheric CO_2 content. CO_2 emissions are specified at historical levels for the period 1870–2000 (Marland et al., 2002) and SRES A2 levels for the period 2000–2100 (IPCC, 2001). Non-CO_2 greenhouse gas concentrations are specified at historical levels for 1870–2000 and SRES A2 levels for 2000–2100 (IPCC, 2001). Land use emissions are taken from Houghton (2003) for the historical period and from the SRES A2 scenario thereafter. There is no change in aerosol forcing. In this scenario, total emissions reach 29 Gt-C yr^{-1} in 2100 from present-day values of 8 Gt-C yr^{-1}. This experiment is called the "fertilization" case in Thompson et al. (2004).

(3) The "0 × sensitivity" case which is identical to the "1 × sensitivity" case except that the radiation model continues to see

Table 1. Changes in global and annual mean model results (decade of 2091–2100 minus 1891–1900)

Experiment	Surface temp. (K)	Precipitation (%)	Water vapour (kg m^{-2}) (%)	Sea ice extent (%)	Sea ice volume (%)	Net flux at TOA (W m^{-2})
Control	−0.35	−0.52	−0.28 (−1.3)	6.4	14.2	0.14
0 × sensitivity	−0.03	−0.03	−0.17 (−0.8)	3.7	0.9	0.03
1 × sensitivity	3.17	5.03	4.87 (22.9)	−26.0	−66.0	1.56
2 × sensitivity	8.00	11.63	13.71 (64.2)	−79.1	−94.5	3.77

TOA = top of the atmosphere.

the pre-industrial atmospheric CO_2 content, yielding a climate sensitivity of 0 K per CO_2 doubling; though the land and ocean carbon cycle models are forced by the predicted atmospheric CO_2 concentration, the physical climate system is not. Our "0 × sensitivity" case is similar to the uncoupled simulations in Cox et al. (2000) and Friedlingstein et al. (2001) except that our simulations are not performed offline.

(4) The "2 × sensitivity" case which is identical to the "1 × sensitivity" case, except that the radiation model sees an amount of CO_2 in the atmosphere that would roughly double the radiative forcing from anthropogenic CO_2. The carbon cycle models use the actual predicted CO_2. Prescribed non-CO_2 greenhouse gas concentrations as seen by the climate system are also modified so that the radiative forcing is approximately twice that of "1 × sensitivity". The methods used to modify the concentrations are given in Appendix A. This would be expected to roughly double the climate sensitivity of the model. We do not expect that the radiative forcing and climate change in 2 × sensitivity will be exactly twice that of the 1 × sensitivity case for the following two reasons. First, we have used approximate formulae to double the forcings in 2 × sensitivity. Secondly our results show that the predicted CO_2 concentration in 2 × sensitivity is slightly higher than in 1 × sensitivity.

The main purpose of these experiments is to provide a set of coupled climate/carbon cycle simulations across which the only varying factor is climate sensitivity to increased atmospheric CO_2 concentrations. By keeping all other factors constant, we simplify the analysis of our results.

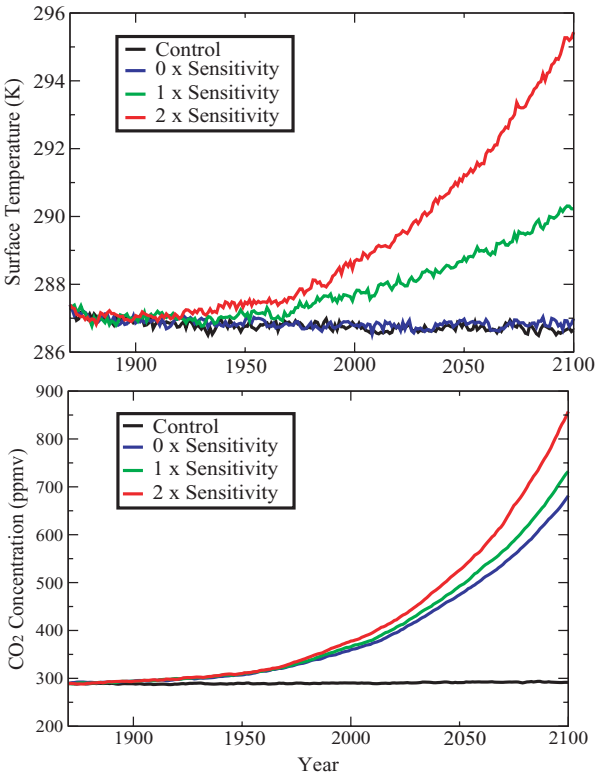

Fig 1. Evolution of global and annual mean surface temperature (upper panel) and atmospheric CO_2 concentration (lower panel). Atmospheric CO_2 concentrations are 51 (176) ppmv higher in the 1 × sensitivity (2 × sensitivity) run than in the 0 × sensitivity run with no climate change.

4. Results

4.1. Climate change

The global and annual mean transient climate responses are listed in Table 1. The response is computed by differencing the averages for AD 2091–2100 and AD 1891–1900. The evolution of global and annual means of surface temperature and atmospheric CO_2 concentration from the four simulations is shown in Fig. 1. Since the climate drifts are small in the control experiment (Fig. 1), we do not subtract the drifts from the other experiments. The climate does not warm in the 0 × sensitivity experiment, warms by about 3.2 K in the 1 × sensitivity experiment, and by 8 K in the 2 × sensitivity case. Because our experiments are transient experiments, the changes in net radiative flux at the top of the atmosphere in the 1 × sensitivity and 2 × sensitivity cases are not close to zero. The net imbalance in the 2 × sensitivity case is 2.4 times that in the 1 × sensitivity case. The warming in the 2 × sensitivity run is 2.5 times that in the 1 × sensitivity run, indicating that the climate response is approximately proportional to radiative forcing. Changes in other global variables such as precipitation, precipitable water and extent of sea ice in the 2 × sensitivity case are also more than twice the changes in the 1 × sensitivity case (Table 1). In the 2 × sensitivity case there is a

decline of nearly 95% of ice volume. We find that the sea ice disappears completely in both hemispheres in their respective summers in that run.

The predicted CO_2 concentration in the 1 × sensitivity and 2 × sensitivity cases reaches 732 and 857 ppmv respectively by 2100. Since the 2 × sensitivity case has higher CO_2 concentrations, it actually has more than twice the CO_2 radiative forcing as in the 1 × sensitivity case. This extra forcing of CO_2 in the 2 × sensitivity case is about 2 W m^{-2} and can explain nearly half of the extra 1.8 K warming. We neglected the negative overlap terms in the radiative forcing formulae for methane and nitrous oxide when we doubled the radiative forcing for these gases (Appendix A). Since these terms decrease the radiative forcing and we have neglected them, the 2 × sensitivity case receives more than twice the radiative forcing of the 1 × sensitivity case due to CH_4 and N_2O also.

The atmospheric CO_2 concentration increases from the pre-industrial level in the 0 × sensitivity and 1 × sensitivity cases by 391 and 442 ppmv, respectively (Fig. 1). The difference is only 51 ppmv between the 0 × sensitivity and 1 × sensitivity cases. Cox et al. (2000) and Friedlingstein et al. (2001) obtained differences of about 250 and 100 ppmv, respectively, in their models. Their year 2100 warmings were 5.5 and 3 K, respectively. The "carbon cycle feedback factor" is defined as the ratio of CO_2 change when climate is changing to the CO_2 change when climate is constant (Friedlingstein et al., 2003). The implied net carbon cycle feedback factor in our simulations is 1.13. The net carbon cycle feedback factors are 1.19 and 1.675 in Friedlingstein et al. (2001) and Cox et al. (2000), respectively. Therefore, our model shows the weakest feedback between climate and carbon cycle among the existing coupled climate and carbon cycle models. However, because of the non-linear dependence of heterotrophic respiration on temperature (Lloyd and Jaylor, 1994), the CO_2 in the 2 × sensitivity case increases by 578 ppmv and the carbon cycle feedback factor increases non-linearly to 1.48. Atmospheric CO_2 concentrations are 176 ppmv higher in the run with 8 K climate change than in the run with no climate change.

4.2. *Land and Ocean carbon fluxes*

The global and annual mean net land and ocean uptakes are shown in Fig. 2. Performing a 5-yr running mean smooths the interannual variability. The model tends to slightly overestimate historical terrestrial carbon uptake estimates for the 1980s and 1990s based on observed intradecadal trends in atmospheric CO_2 and O_2 (Prentice et al., 2001). The land uptake increases monotonically with time in the 0 × sensitivity case and it reaches values larger than 10 Gt-C yr^{-1}, by 2100, more than a third of the emission rate at that time. The effect of CO_2 fertilization is probably exaggerated in these simulations because we do not consider factors other than limitation by sunlight, water and carbon dioxide. Inclusion of other factors, such as nitrogen or phosphate limitation might diminish the magnitude of the response to added CO_2 (Hungate et al., 2003). Compared with similar models, IBIS also tends to simulate a higher fertilization effect (McGuire et al., 2001).

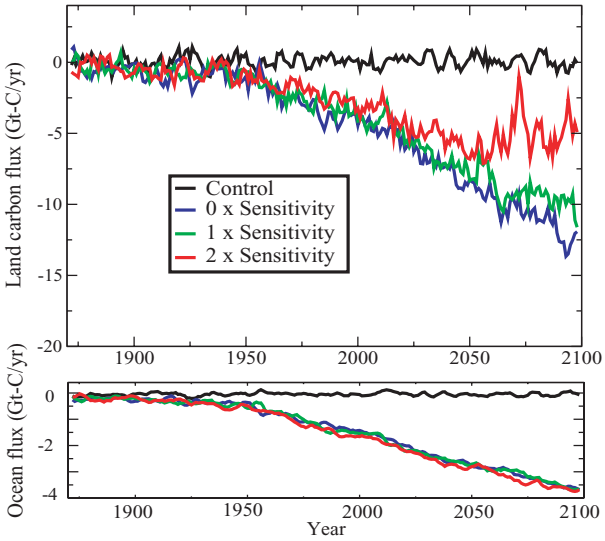

Fig 2. Evolution of the 5-yr running mean of global, annual flux of carbon from land to atmosphere (upper panel) and from ocean to atmosphere (lower panel). Negative values represent fluxes into land and ocean. Land fluxes are reduced to half when the climate change is doubled, and ocean fluxes are insensitive to climate change in our model.

Land uptake of carbon is similar in the 0 × sensitivity and 1 × sensitivity cases up to 2070; after this the 1 × sensitivity case takes up less carbon than the 0 × sensitivity case because of increase in heterotrophic (soil microbial) respiration (Fig. 3). We find that the spatial pattern of soil respiration correlates strongly with soil carbon pools. The spatial patterns of surface temperature and precipitation are also important. It is the covariance of these changes with the size of respirable carbon pools that controls the magnitude of respiration. The larger warming in the 2 × sensitivity case results in significantly increased soil microbial respiration and reduced land uptake of carbon (Fig. 3); soil carbon content declines after the year 2050. The land biosphere takes up less than half the carbon it takes up in the 0 × sensitivity case after 2050 (Fig. 2). Interannual variability increases in all cases after 2050, because of the larger carbon pools in the terrestrial biosphere.

Our results are in agreement with Friedlingstein et al. (2001), who obtained reduced land uptake with climate change in the IPSL model when CO_2 concentrations were increasing at 1% per annum. However, our results are in sharp contrast to Cox et al. (2000), who showed that land becomes a source of carbon around the year 2050 when they forced their model HadCM3 with the IS92a scenario. With the HadCM3 model, a drying and warming of the Amazon initiates a collapse of the tropical forest followed by large releases of soil carbon. Such a loss of vegetation biomass and soil carbon content does not occur in our

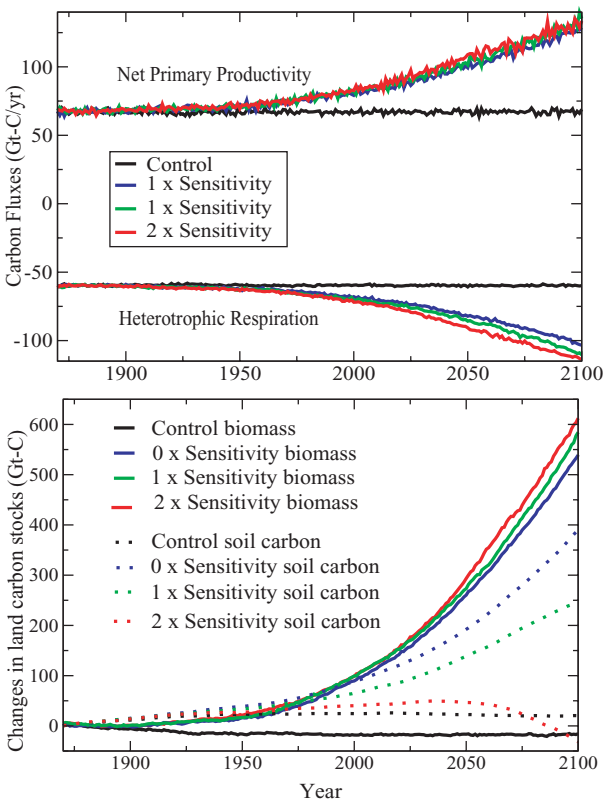

Fig 3. Evolution of net primary productivity (NPP) and heterotrophic (soil microbial) respiration (upper panel) and changes in vegetation biomass and soil carbon content (lower panel). The increase in biomass is similar in 0 ×, 1 × and 2 × sensitivity experiments because the NPPs are similar. Soil carbon change the in 1 × sensitivity case is smaller than in the 0 × sensitivity case because of increase in soil microbial respiration. Further increases in soil respiration in the 2 × sensitivity case leads to declines in soil carbon content after 2050.

1 × sensitivity simulation (Fig. 3). The increase of global mean NPP with time is very similar in the 0 ×, 1 × and 2 × sensitivity experiments. We do not see any sign of declines in biomass with warming even in the 2 × sensitivity case (Fig. 3). Actually, NPP and biomass are slightly higher in the 2 × sensitivity than in the 0 × and 1 × sensitivity cases, because the 2 × sensitivity case has the highest atmospheric CO_2 concentration. NPP and biomass are responding more strongly to CO_2 fertilization than to warming. In the1 × sensitivity case, both vegetation biomass and soil carbon are increasing and the warming is only 3.2 K (as opposed to 5.5 K in HadCM3). In the 2 × sensitivity case, soil carbon is decreasing because of increased respiration due to an 8 K warming, but biomass still keeps increasing (Fig. 3).

For the 0 × sensitivity run, ocean CO_2 uptake also shows a monotonic increase up to 2100 because of rising atmospheric CO_2 (Fig. 2). The uptake reaches about 3.5 Gt-C yr^{-1}—only a third of the land uptake. This may be an underestimate, as the model tends to underestimate historical ocean carbon uptake estimates based on observed intradecadal trends in atmospheric CO_2 and O_2 (Prentice et al., 2001) and model results from OCMIP (Orr and Dutay, 1999; Orr et al., 2001). The larger increases in atmospheric CO_2 in the 1 × sensitivity and 2 × sensitivity runs compared with the 0 × sensitivity run would be expected to drive an increased flux of CO_2 into the ocean. However, this is not seen (Fig. 2), in part because increasing ocean temperature results in lower CO_2 solubility. The global mean ocean surface temperature increases by 2.1 K in the 1 × sensitivity run and by 6 K in the 2 × sensitivity run, offsetting increases in uptake due to the further increases in atmospheric CO_2. Surface warming also causes increased thermal stratification, which inhibits downward transport of anthropogenic carbon (Sarmiento and Le Quere, 1996; Sarmiento et al., 1998).

In the HadCM3 and IPSL simulations, climate change in the 1 × sensitivity simulations produced less ocean carbon uptake than in the 0 × sensitivity simulations (Cox et al., 2000; Friedlingstein et al., 2003). Our ocean model results are more similar to those of Cox et al. (2000) (uptake in HadCM3 was ∼5 Gt-C yr^{-1}) than those of Friedlingstein et al. (2001). In the IPSL simulation (Friedlingstein et al., 2001), the ocean uptake was ∼10 Gt-C yr^{-1} in the 0 × sensitivity case due to strong convection in the Southern Ocean; this uptake decreased moderately in their 1 × sensitivity simulation.

4.3. *Fate of anthropogenic emissions*

Under the SRES A2 scenario, total emissions reach 29 Gt-C yr^{-1} by 2100. Cumulative anthropogenic emissions for the period 1870 to 2100 amount to 2200 Gt-C. The amounts taken up by land and ocean are shown in Fig. 4. In the 0 × sensitivity case, land takes up 1031 Gt-C, nearly 50% of the emissions (Fig. 4a). The uptake is reduced to 919 and 629 Gt-C in the 1 × sensitivity and 2 × sensitivity runs, respectively. Therefore, land uptake decreases from 47 to 29% (1031 to 629 Gt-C) of the total emissions as the global temperature change increases from 0 to 8 K in our model. The HadCM3 modelling study showed a range of –5 to 34% (−100 to 650 Gt-C) of the 1900 Gt-C emissions of the IS92a scenario for the same temperature range (Cox et al., 2000; Freidlingstein et al., 2003). Therefore, there is a large range of model projections of future land uptake in current coupled climate/carbon models. Friedlingstein et al. (2003) demonstrated that the climate impact on the land carbon cycle is mainly responsible for the large difference in the overall response of the IPSL and HadCM3 models.

The total ocean uptake in our 0 × sensitivity, 1 × sensitivity and 2 × sensitivity cases differs little (Fig. 4b). The net uptake over the period 1870–2100 is around 350 Gt-C in all the runs. Therefore, future ocean carbon uptake appears to be relatively insensitive to uncertainty in climate sensitivity in our model for specified CO_2 emission scenarios. In agreement with our results, Cox et al. (2000) and Friedlingstein et al. (2001) obtained only modest sensitivity of the ocean carbon uptake to climate change in the HadCM3 and IPSL models.

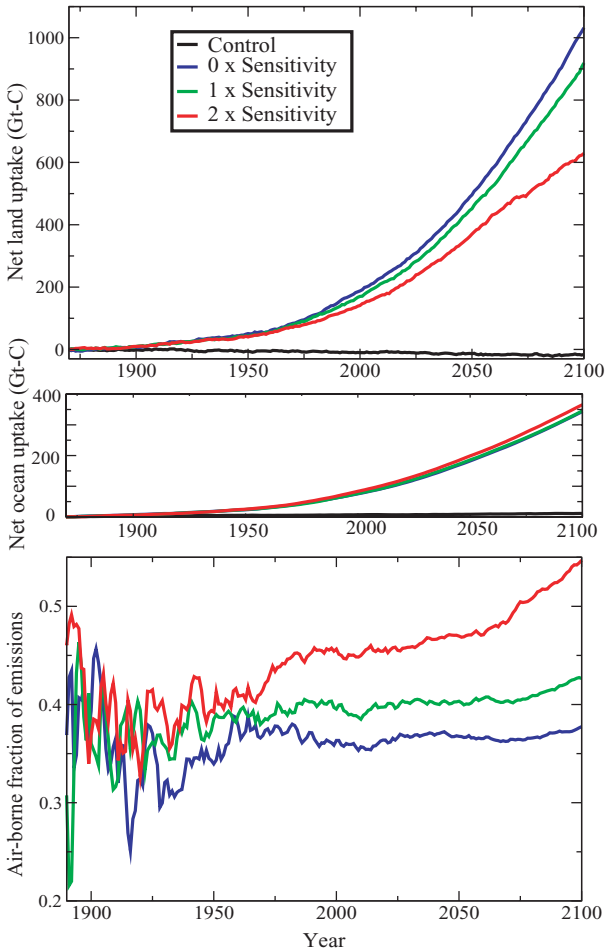

Fig 4. Evolution of cumulative carbon uptakes by land (upper panel) and oceans (middle panel) since the pre-industrial period. The air-borne fraction of cumulative emissions is shown in the bottom panel. Our results suggest a large range in land uptake, and air-borne fraction, and little change in ocean uptake over the 0–8 K range of global warming.

The fraction of the cumulative anthropogenic emissions that remains in the atmosphere at any time since year 1870 depends on the climate change (Fig. 4c). Since the averaging time interval increases with time, the fractions exhibit little variability in the later periods and the curves become smooth towards the end of simulations. The fractions from all the runs are close to each other until 1970. After that, they diverge from each other. In the 0 × sensitivity case, only 37% of the total emissions remain in the atmosphere by 2100. This fraction reaches 43% and 55% in the 1 × sensitivity and 2 × sensitivity cases, respectively. Therefore, the fraction of emissions that remains in the atmosphere increases with warming primarily because the land uptake declines with warming.

4.4. Changes in distribution of vegetation

IBIS simulates the present-day distribution of vegetation fairly realistically (Foley et al., 1996) when forced with the observed climate. Dominant vegetation distributions from our simulations for the period 2071–2100 are shown in Fig. 5. We use kappa statistics (Monsrrud, 1990) to compare maps of vegetation distributions. Kappa takes on a value of 1 with perfect agreement. It has a value close to zero when the agreement is approximately the same as would be expected by chance. A kappa value of 0.47 (fair agreement; Landis and Koch, 1977) is obtained for a comparison of IBIS simulated vegetation and observations (Foley et al., 1996).

Global comparison of control vegetation distributions with distributions from the 0 ×, 1 × and 2 × sensitivity runs gives kappa values of 0.80 (very good agreement), 0.54 (good) and 0.40 (fair) respectively. The high kappa value for comparison between the control and 0 × sensitivity cases suggests that atmospheric CO_2 changes alone have a weaker influence on changing the vegetation distribution than climate change; the 0 × sensitivity run has no climate change but it has carbon cycle changes due to fossil fuel emissions. However, as the global warming increases, the vegetation distribution changes dramatically; the kappa value decreases from 0.8 to 0.4 when the warming increases from 0 to 8 K.

In terms of area occupied by different vegetation types, tropical and temperate forests expand significantly with global warming (Fig. 5; Table 2). The area covered by these forests increases from about 40% in the control case to nearly 60% of the land area in the 2 × sensitivity case. In general there is a migration of tropical, temperate and boreal forests poleward with warming, leading to significant declines in the area occupied by tundra and polar deserts (land ice) in the 2 × sensitivity run. We caution that climate change and CO_2 fertilization could also have an impact on ecosystem goods and services not represented by our terrestrial ecosystem model, such as species abundance and competition, habitat loss, biodiversity and other disturbances (Root and Schneider, 1993).

5. Discussion

The climate model used here has equilibrium climate sensitivity to increased CO_2 (2.1 K per doubling) that is at the lower end of the range of the general model population (IPCC, 2001). In order to address the dependence of carbon cycle feedback on climate sensitivity we investigated the sensitivity of this positive feedback for a range of equilibrium climate sensitivities to increased atmospheric CO_2 content; nominally, 0, 2 and 4 K per doubling of atmospheric CO_2 content. With the SRES A2 emission scenarios, this produces a simulated year 2100 global warming ranging from 0 to 8 K. We find that the land biosphere takes up less carbon with higher climate sensitivity, and this is not compensated for by increased ocean carbon uptake. Thus, the higher climate sensitivity simulations are warmer both because of increased sensitivity to added CO_2 and because more CO_2 remained in the atmosphere.

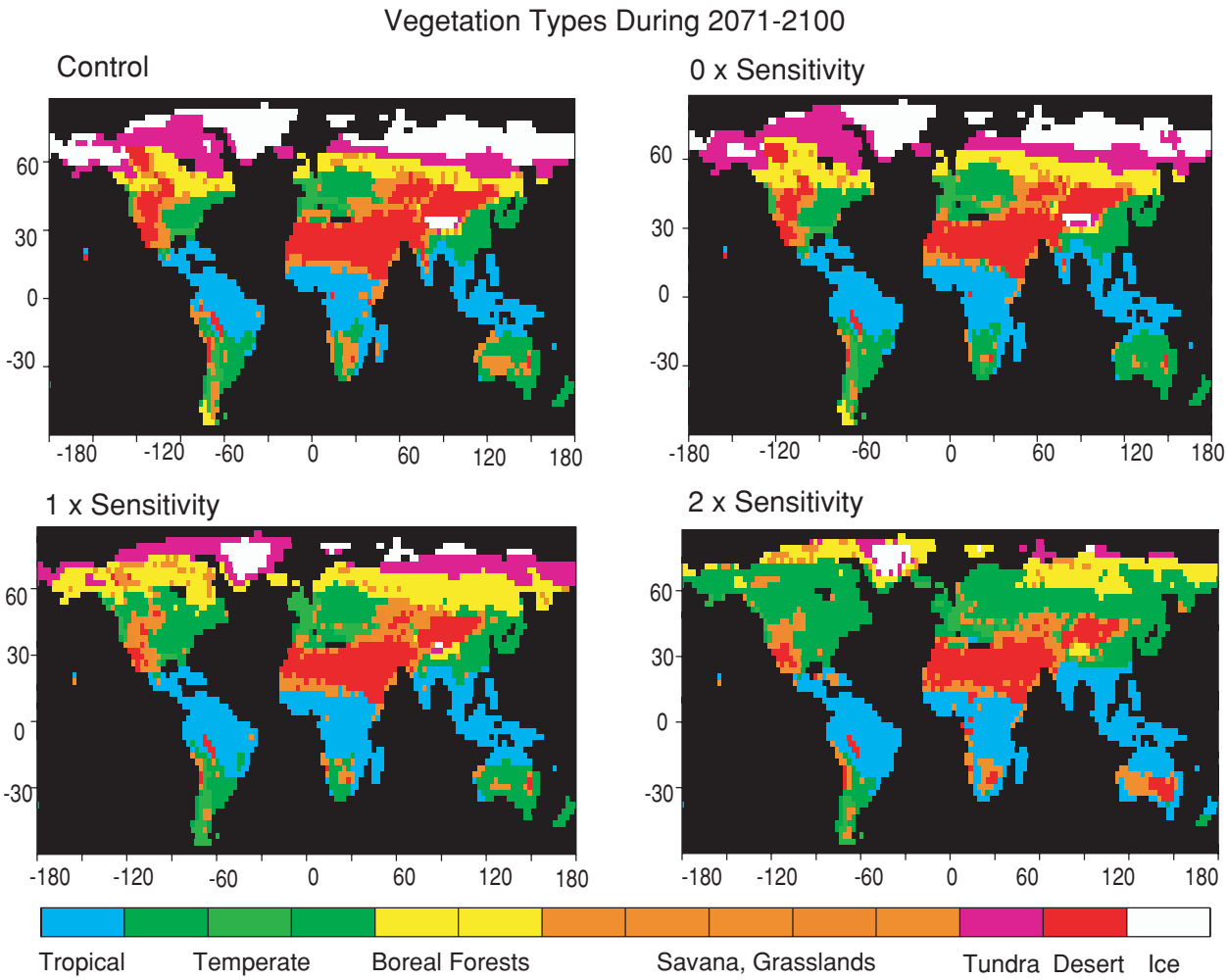

Fig 5. Vegetation distributions in our simulations. Antarctica is not shown. The area covered by tropical and temperate forests increases dramatically when global warming increases from 0 to 8 K. There is a also migration of tropical, temperate and boreal forests poleward with warming, leading to significant declines in the area occupied by tundra and polar deserts (land ice) in the 2 × sensitivity run.

Table 2. Fraction of land area occupied by vegetation types during 2071–2100

Vegetation type	Control	0 × sensitivity	1 × sensitivity	2 × sensitivity
Tropical forests	22.2	24.2	24.6	30.3
Temperate forests	19.3	22.7	24.3	29.0
Boreal forests	6.7	8.2	10.6	5.8
Savannah, grasslands and shrublands	12.5	8.5	11.8	12.9
Tundra	6.9	8.8	6.5	2.6
Desert	16.4	14.5	12.3	13.4
Polar desert	16.0	13.1	7.9	6.0

In our model, the carbon cycle feedback factor increases from 1.13 to 1.48 when global warming increases from 3.2 to 8 K. The cumulative land uptake varies between 29 and 47% of the total emissions for a 0–8 K range in temperature change. The ocean uptake (16%) shows almost no change at all. The fraction of the total emissions that remain in the atmosphere ranges from 37 to 55% under different amount of climate changes. Atmospheric CO_2 concentrations are 176 ppmv higher in the run with 8 K climate change than in the run with no climate change. Our results are in agreement with other modelling studies that concluded that the climate impact of the land carbon cycle is mainly responsible for the

modelling uncertainty in the projection of future atmospheric CO_2 concentrations.

In contrast to Cox et al. (2000) but in agreement with Friedlingstein et al. (2001), our land carbon cycle model does not become a net source of carbon to the atmosphere even when the warming is as high as 8 K. In HadCM3 (Cox et al., 2000), vegetation carbon in the Amazon begins to decline, as a drying and warming of Amazonia initiates loss of forest. Such a loss of vegetation biomass does not occur in our simulations. In our model, soil carbon does show declines by 2100 for an 8 K global warming. This results in reduced land uptake of carbon. However, the vegetation biomass keeps increasing.

The high sensitivity of our terrestrial biosphere model to CO_2 may be associated with the lack of nutrient cycles (e.g. nitrogen, phosphorus, etc.). In the real world, as opposed to our model, CO_2-fertilized ecosystems may run into nutrient limitations. Changes in nitrogen availability are important to the carbon cycle through changes in availability of plant nutrients (Schimel, 1998; Nadelhoffer et al., 1999; Hungate et al., 2003). Models that include nitrogen limitation show less sensitivity of CO_2 fluxes for changes in atmospheric CO_2 (Cramer et al., 2001).

Thompson et al. (2004) bracketed the uncertainty in land uptake due to nitrogen/nutrient limitations of CO_2 fertilization. They showed that the atmospheric CO_2 concentrations are 336 ppmv (40%) lower in the fully fertilized case than the fertilization-capped case. Here we have shown how land fluxes may depend on climate sensitivity to CO_2 itself. The sensitivity to nitrogen/nutrient limitation obtained in Thompson et al. (2004) is about twice of what we find for a 0–8 K range in global warming.

In order to explore the full range of carbon cycle feedback factors for the global warming range considered here and nitrogen/nutrient limitations considered in Thompson et al. (2004), we performed three additional experiments in which the CO_2 fertilization for the land biosphere was capped at year 2000 levels as in Thompson et al. (2004). These experiments are labelled as saturation cases. Experiments without this capping (unlimited fertilization) are called fertilization cases. The carbon cycle feedback factors for all the experiments are listed in Table 3. By definition (Friedlingstein et al., 2001), the feedback factor is unity for the $0 \times$ sensitivity fertilization case. The model shows a strong sensitivity to both climate sensitivity and nitrogen/nutrient limitations; the feedback factor reaches a high value of 2.75 when CO_2 fertilization is capped at year 2000 levels and when climate sensitivity is doubled. The CO_2 level in the atmosphere in this case at year 2100 is doubled when compared with the case with full CO_2 fertilization and no climate change. The ranges for carbon cycle feedback factor and year 2100 atmospheric CO_2 are 1.0–2.75 and 681–1365 ppmv, respectively.

Table 3. Carbon cycle feedback factors for various scenarios. Bracketed values are year 2100 values of CO_2 in ppmv

	$0 \times$ sensitivity	$1 \times$ sensitivity	$2 \times$ sensitivity
Fertilization	1.0 (681)	1.13 (732)	1.48 (857)
Saturation	1.71 (960)	2.05 (1068)	2.75 (1365)

The results of this fully coupled climate–carbon model show that the carbon cycle feedback factor and the amount of anthropogenic CO_2 in the atmosphere at the end of the 21st century will probably be sensitive to terrestrial carbon cycle processes and climate sensitivity about which we are uncertain at present. The major uncertain carbon cycle processes are CO_2 fertilization, nitrogen/nutrient limitations and acclimation of soil microbiology to the higher temperatures (Kirschbaum, 2000; Tjoelker et al., 2001). These uncertainties could perhaps be narrowed with investigation of carbon dynamics across a broad range of ecosystems and climate regimes, often including manipulation experiments, and redoubled efforts to represent those dynamics in climate models. Development of models including known limiting factors, like acclimation and explicit nitrogen/nutrient cycling, will be important to narrow down the uncertainty. Without this research, we cannot predict the amount of anthropogenic carbon that can be sequestrated in the land biosphere.

6. Acknowledgments

This work was performed under the auspices of the U.S. Department of Energy by the University of California Lawrence Livermore National Laboratory under contract no W-7405-Eng-48.

7. Appendix A

The greenhouse gases used in our model are CO_2, CH_4, N_2O, CFC11 and CFC12. The functional dependence of radiative forcing on greenhouse gases is taken from IPCC (1997). Suppose we want N times the actual forcing. For CO_2, the forcing F is calculated as

$$F = K \ln(C(t)/C_0),$$

where C is the predicted concentration of CO_2 and C_0 is the pre-industrial concentration. K is a constant that varies with the model. We multiply C by the ratio $(C/C_0)^{N-1}$ for performing the radiation calculations in the GCM to ensure approximately N times the actual forcing.

Omitting the overlap terms, the radiative forcing for CH_4 and N_2O is given by $F = k(\sqrt{M} - \sqrt{M_0})$ where M is the concentration, M_0 is the pre-industrial concentration and $k =$ 0.036 for CH_4 and 0.14 for N_2O. We multiply M by $[N + (1 - N)\sqrt{C_0/C}]^2$ to increase the radiative forcing by N times. Since the forcing of CFC11 and CFC12 varies linearly with their concentrations, we just multiply their concentrations by N to get N times the actual forcing.

References

Ball, J. T., Woodraw, I. E. and Berry, J. A. 1986. A model predicting stomatal conductance and its contribution to the control of photosynthesis under different environmental conditions. In: *Progress in Photosynthesis Research* Volume 4 (ed. J. Biggins). Martinus Nijhoff, Zoetermeer, The Netherlands, 221–224.

Braswell, B. H., Schimel, D. S., Linder, E. and Moore, B. 1997. The response of global terrestrial ecosystems to interannual temperature variability. *Science* **278**, 870–872.

Cao, M. and Woodward, F. I. 1998. Dynamic responses of terrestrial ecosystem carbon cycling to global climate change. *Nature* **393**, 249–252.

Collatz, G. J., Ball, J. T., Grivet, C. and Berry, J. A. 1991. Physiological and environmental regulation of stomatal conductance, photosynthesis, and transpiration: a model that includes a laminar boundary layer. *Agr. Forest Meteorol.* **53**, 107–136.

Collatz, G. J., Ribas-Carbo, M. and Berry, J. A. 1992. Coupled photosynthesis-stomatal conductance model for leaves of C_4 plants. *Aust. J. Plant Physiol.* **19**, 519–538.

Cox, P. M., Betts, R. A., Jones, C. D., Spall, S. A. and Totterdell, I. J. 2000. Acceleration of global warming due to carbon-cycle feedbacks in a coupled model. *Nature* **408**, 184–187.

Cramer, W., Bondeau, A., Woodward, F. I., Prentice, I. C., Betts, R. A. and co-authors. 2001. Global response of terrestrial ecosystem and function to CO2 and climate change: results from six dynamic global vegetation models. *Global Change Biol.* **7**, 357–373.

Dukowicz, J. K. and Smith, R. D. 1994. Implicit free-surface method for the Bryan–Cox–Semtner ocean model. *J. Geophys. Res.* **99**, 7991–8014.

Farquhar, G. D., von Caemmerer, S. and Berry, J. A. 1980. A biogeochemical model of photosynthetic CO_2 assimilation in leaves of C_3 plants. *Planta* **149**, 78–90.

Foley, J. A., Prentice, I. C., Ramankutty, N., Levis, S., Pollard, D. and co-authors. 1996. An integrated biosphere model of land surface processes, terrestrial carbon balance and vegetation dynamics. *Global Biogeochem. Cycles* **10**, 603–628.

Friedlingstein, P., Bopp, L., Clais, P., Dufresne, J.-L., Fairhead, L. and co-authors. 2001. Positive feedback between future climate change and the carbon cycle. *Geophys. Res. Lett.* **28**, 1543–1546.

Friedlingstein, P., Dufresne, J.-L., Cox, P. M. and Rayner, P. 2003. How positive is the feedback between climate change and the carbon cycle? *Tellus* **55B**, 692–700.

Fung, I., Field, C. B., Berry, J. A., Thompson, M. V., Randerson, J. T. et al. 1997. Carbon 13 exchanges between the atmosphere and biosphere. *Global Biogeochem. Cycles* **11**, 507–533.

Houghton, R. 2003. Revised estimates of the annual net flux of carbon to the atmosphere from changes in land use and land management 1850–2000. *Tellus* **55B**, 378–390.

Hungate, B. A., Dukes, J. S., Shaw, M. R., Luo, Y. and Field, C. B. 2003. Nitrogen and climate change. *Science* **302**, 1512–1513.

IGBP Terrestrial Carbon Working Group. 1998. The terrestrial carbon cycle: implications for the Kyoto Protocol. *Science* **280**, 1393–1394.

IPCC (Intergovernmental Panel on Climate Change) 1997. *An Introduction to Simple Climate Models used in the IPCC Second Assessment Report*. IPCC Technical Paper II (eds. J. T. Houghton, L. G. M. Filho, D. J. Griggs and K. Masket). IPCC, Geneva, Switzerland.

IPCC (Intergovernmental Panel on Climate Change) 2001. *Climate Change 2001, The Scientific Basis*. Cambridge University Press, New York.

Joos, F., Prentice, I. C., Sitch, S., Meyer, R., Hooss, G. and co-authors. 2001. Global warming feedbacks on terrestrial carbon uptake under the Intergovernmental Panel on Climate Change (IPCC) emission scenarios. *Global Biogeochem. Cycles* **15**, 891–907.

Kiehl, J. T., Hack, J. J., Bonan, G. B., Boville, B. Y., Briegleb, B. P. et al. 1996. *Description of the NCAR Community Climate Model (CCM3)*. NCAR Technical Note, NCAR/TN-420+STR. National Center for Atmospheric Research, Boulder, Colorado.

King, A. W., Post, W. M. and Wullschleger, S. D. 1997. The potential response of terrestrial carbon storage to changes in climate and atmospheric CO_2. *Climate Change* **35**, 199–227.

Kirschbaum, M. U. F. 2000. Will changes in soil organic carbon act as a positive or negative feedback on global warming? *Biogeochemistry* **48**, 21–51.

Kucharik, C. J., Foley, J. A., Delire, C., Fisher, V. A., Coe, M. T. et al. 2000. Testing the performance of a dynamic global ecosystem model: water balance, carbon balance, and vegetation structure. *Global Biogeochem. Cycles* **14**(3), 795–825.

Landis, J. R. and Koch, G. G. 1977. The measurement of observer agreement for categorical date. *Biometrics* **33**, 159–174.

Lloyd, J. and Jaylor, J. A. 1994. On the temperature dependence of soil respiration. *Functional Ecol.* **8**, 315–323.

Maier-Reimer, E. 1993. Biogeochemical cycles in an ocean general-circulation model—preindustrial tracer distributions. *Global Biogeochem. Cycles* **7(3)**, 645–677.

Maltrud, M. E., Smith, R. D., Semtner, A. J. and Malone, A. J. 1998. Global eddy-resolving ocean simulations driven by 1985–1995 atmospheric winds. *J. Geophys. Res.* **103**, 30 825–30 853.

Marland, G., Boden, T. and Andres, R. 2002. *Global, regional, and national annual CO2 emissions from fossil-fuel burning, cement production and gas flaring: 1751–1999*. CDIAC NDP-030. Carbon Dioxide Information Analysis Center, Oak Ridge National Laboratory, Oak Ridge, TN.

McGuire, A. D., Sitch, S., Clein, J. S., Dargaville, R., Esser, G. and co-authors. 2001. Carbon balance of the terrestrial biosphere in the twentieth century: analyses of CO_2, climate and land-use effects with four process-based ecosystem models. *Global Biogeochem. Cycles* **15**, 183–206.

Meehl, G. A., Washington, W. M., Arblaster, J. M. and Hu, A. 2004. Factors affecting climate sensitivity in global coupled models. *J. Climate*, **17**, 1584–1596.

Monserud, R. A. 1990. *Methods for comparing global vegetation maps*. IIASA WP-90–40. International Institute for Applied Systems Analysis, Laxenburg, Austria.

Nadelhoffer, K. J., Emmett, B. A. and Gundersen, P. 1999. Nitrogen makes a minor contribution to carbon sequestration in temperate forests. *Nature* **398**, 145–148.

Najjar, R. G. and Orr, J. C. 1999. *Biotic How-To, Revision 1.7*. Ocean Carbon-cycle Model Intercomparison Project (OCMIP). http://www.ipsl.jussieu.fr/OCMIP/phase2/simulations/Biotic/HOWTO-Biotic.html

Orr, J. C. and Dutay, J.-C. 1999. OCMIP mid-project workshop. *Research GAIM Newsletter* **3**, 4–5.

Orr, J. C., Maier-Raimer, E., Mikolajewicz, U., Monfray, P., Sarmiento, J. L. et al. 2001. Estimates of anthropogenic carbon uptake from

four 3-D global ocean models. *Global Biogeochem. Cycles* **15**, 43–60.

Prentice, I. C., Farquhar, G. D., Fasham, M. J. R., Goulden, M. L., Heimann, M. et al. 2001. *Climate Change 2001: The Scientific Basis: Contribution of Working Group I to the Third Assessment Report of the IPCC* (eds J. T. Houghton et al.). Cambridge University Press, Cambridge, pp. 183–237.

Prentice, I. C., Heimann, M. and Sitch, S. 2000. The carbon balance of the terrestrial biosphere; ecosystem models and atmospheric observations. *Ecol. Applic.* **10**(6), 1553–1573.

Root, T. L. and Schneider, S. H. 1993. Can large scale climatic models be linked with multiscale ecological studies? *Conserv. Biol.* **7(2)**, 256–270.

Sarmiento, J. L., Hughes, T. C., Stouffer, R. J. and Manabe, S. 1998. Simulated response of the ocean carbon cycle to anthropogenic climate warming. *Nature* **393**, 245–249.

Sarmiento, J. L. and Le Quere, C. 1996. Oceanic carbon dioxide uptake in a model of century-scale global warming. *Science* **274**, 1346–1350.

Schimel, D. S. 1998. The Carbon equation. *Nature* **393**, 208–209.

Thompson, S., Govindasamy, B., Mirin, A., Caldeira, K., Delire, C. et al. 2004. Quantifying the effects of CO_2-fertilized vegetation on future climate. *Geophys. Res. Lett.* **31**, L23211.

Tian, R. C., Vézina, A. F., Legendre, L., Ingram, R. G., Klein, B. et al. 2000. Effects of pelagic food-web interactions and nutrient remineralization on the biogeochemical cycling of carbon: a modeling approach. *Deep-Sea Res.* **47**, 637–662.

Tjoelker, M. G., Oleksyn, J. and Reich, P. B. 2001. Modelling respiration of vegetation: evidence for a general temperature-dependent $Q(10)$. *Global Change Biol.* **7**, 223–230.

UNFCCC. 1997. The Kyoto Protocol to the United Nations Framework Convention on Climate Change, http://www.unfcc.int/resource/convkp.html.

Washington, W. M., Weatherly, J. W., Meehl, G. A., Semtner, A. J. Jr, Bettge, T. W. et al. 2000. Parallel Climate Model (PCM) control and transient simulations. *Clim. Dynam.* **16**, 755–774.

Wolf-Gladrow, D. and Riebesell, U. 1997. Diffusion and reactions in the vicinity of plankton: a refined model for inorganic carbon transport. *Mar. Chem.* **59**, 17–34.